Available online at www.sciencedirect.com
SCIENCE DIRECT®
Catalysis Today 97 (2004) 181–188
CATALYSIS TODAY
www.elsevier.com/locate/cattod

A study of ethanol dehydrogenation reaction in a palladium membrane reactor

Wen-Hsiung Lin, Hsin-Fu Chang*

Department of Chemical Engineering, Feng Chia University, Taichung, Taiwan 407, ROC

Received 18 November 2003; received in revised form 11 February 2004; accepted 25 March 2004
Available online 11 September 2004

Abstract

Palladium alloy membranes were prepared by sequential electroless plating steps on porous stainless steel. In this communication ethanol dehydrogenation to produce acetaldehyde and hydrogen was investigated in a palladium-based membrane reactor. Generally, the ethanol conversion increased with increasing flow rates of sweep gas and decreasing transmembrane pressures. The effect of sweep-gas flow rates on enhancing H_2 fluxes was remarkable at higher temperatures. The recovery of H_2 increased with increasing the flow rate of sweep gas, the transmembrane pressure and the temperature. The Pd-based dense membrane reactors gave a conversion higher than the thermodynamic equilibrium value for the dehydrogenation of ethanol.

Keywords: Sequential electroless plating; Pd–Ag/PSS membrane reactor; Ethanol dehydrogenation; Sweep gas

1. Introduction

The dehydrogenation of saturated hydrocarbons to alkenes, which is used as an intermediate in the production of new fuels and fuel additives, has gained more importance in chemical industry in the past several decades. Membrane reactors are processing chemical reaction and separation in one unit and especially, being selective to one or more of the product, can be used to improve the yields of thermodynamically limited reactions. When conducting dehydrogenation reactions, which are normally endothermic, palladium based membrane reactor technologies appear promising since the selective removal of high-purity hydrogen would inevitably tend to shift the equilibrium toward increased product yields. Palladium-based membranes are commercially used for hydrogen purification, and to some extent for improving conversions in dehydrogenation reactions by shifting the reaction equilibrium [1–5].

Silver is added to palladium to prevent hydrogen embrittlement that takes place below near 300 °C for pure palladium and to increase the hydrogen flux. The enhancement of the H_2 permeability by alloying the Pd with Ag or other elements has been well established [6]. The optimum silver concentration is in the region of 23 wt.% silver [7–8].

Electroless plating appears to be quite attractive due to the possibility of uniform deposition on complex shapes and large substrate areas, hardness of the deposited film, and very simple equipment. Electroless plating has been used to produce Pd and Pd-alloy membranes on a wide variety of supports, which include porous glass [9–11], alumina [12–14], and porous stainless steel [15–16]. Yeung and Varma [17] prepared Pd–alumina composite membrane by using osmotic pressure for the manipulation of the microstructure, porosity, and thickness of the deposited metal. The main advantages of porous stainless steel (PSS) supports over porous ceramics and Vycor glass are the resistance to crack and the simplicity of module construction. Additionally, the thermal expansion coefficient of stainless steel is almost identical to that of palladium, insuring good mechanical properties of the composite membrane during thermal cycling.

In this study, we have prepared the Pd-based membrane reactor made of stainless steel designed for performing the ethanol dehydrogenation. We have also investigated the effects on ethanol conversion by partial removal of hydrogen

* Corresponding author. Tel.: +886 4 24517545; fax: +886 4 24510890.
E-mail address: hfchang@fcu.edu.tw (H.-F. Chang).

0920-5861/$ – see front matter © 2004 Elsevier B.V. All rights reserved.
doi:10.1016/j.cattod.2004.03.068

from the reaction side as a result of permeation through the Pd-based membrane, and by the variation of the fluxes of sweep nitrogen gas.

2. Experimental

2.1. Preparation of Pd-Based/PSS composite membranes

Pd and Pd–Ag/PSS membranes were prepared using conventional electroless plating. Prior to the membrane preparation, dirt and grease in the porous (average pore size ca. 4 μm from pore size distribution) SS-316L tube support (effective area ca. 20 cm^2; Mott Metallurgical Corporation) were removed by cleaning successively with dilute sodium hydroxide solution, dilute phosphate acid solution and deionised water. The activation procedure consisted of the two-step immersion sequence, which was in acidic $SnCl_2$ solution (1 g/L) followed by acidic $PdCl_2$ solution (1 g/L). After surface activation, palladium deposition was performed first in a 4 g $Pd(NH_3)_4Cl_2$/L plating bath lasted 1 h at 333 K, moderate N_2H_4 being added. Silver deposition in a 0.5 g $AgNO_3$/L plating bath was then performed for 1 h under similar conditions. The plating step was repeated until expected thickness of the membrane was reached. After each deposition, the membrane was rinsed with deionised water, then dried in an oven at 393 K for 2 h. Finally, the membrane was sintered and annealed in hydrogen at atmospheric pressure for more than 18 h [18].

2.2. Gas permeation measurement

Permeation measurements were conducted on the Pd and Pd–Ag/PSS membranes at elevated temperature (623–873 K) and pressures (differences up to 1 MPa). The schematic diagram of gas permeation apparatus was shown in Fig. 1. The assembly of permeability testing consisted of gas cylinders, a membrane reactor (Fig. 2, no catalyst packed), a gas chromatograph, a back-pressure regulator, and pressure gauges. The upstream pressure was controlled by the back-pressure regulator, whereas the downstream of gas vented to air. Prior to the hydrogen permeation measurement, the flow system was preheated to the setting temperature in the nitrogen atmosphere. The permeation rates of individual gases (hydrogen and nitrogen) were measured at atmospheric pressure and ambient temperature by a soap-bubble flowmeter.

2.3. Ethanol dehydrogenation with Pd–Ag/PSS composite membrane reactor

The dehydrogenation of ethanol, $CH_3CH_2OH \rightarrow CH_3CHO + H_2$, occurred in the shell side of a palladium membrane reactor in which a dehydrogenation catalyst was packed. The product hydrogen permeating through the membrane into the inner tube was collected. The dehydrogenation reactor was placed inside a thermostat as shown in Fig. 2. In between the stainless shell and the membrane tube Cu–Zn/Al_2O_3 catalyst powders were uniformly mixed with silica powder. Ethanol was fed to an evaporator with a high-pressure syringe pump, vaporized and sent to the catalyst bed of the reactor. The reaction pressure was controlled in the range of 2–11 bar with a back-pressure regulator.

Catalytic activity was measured in terms of ethanol conversion, defined as:

$$X = \frac{F^{\text{in}}_{\text{ethanol}} - F^{\text{out}}_{\text{ethanol}}}{F^{\text{in}}_{\text{ethanol}}}$$

Products distributions were evaluated through their selectivity and selectivity of specie i was defined as:

$$S_i = \frac{F^{\text{out}}_i}{F^{\text{in}}_{\text{ethanol}} - F^{\text{out}}_{\text{ethanol}}}$$

where F is the molar flow rate.

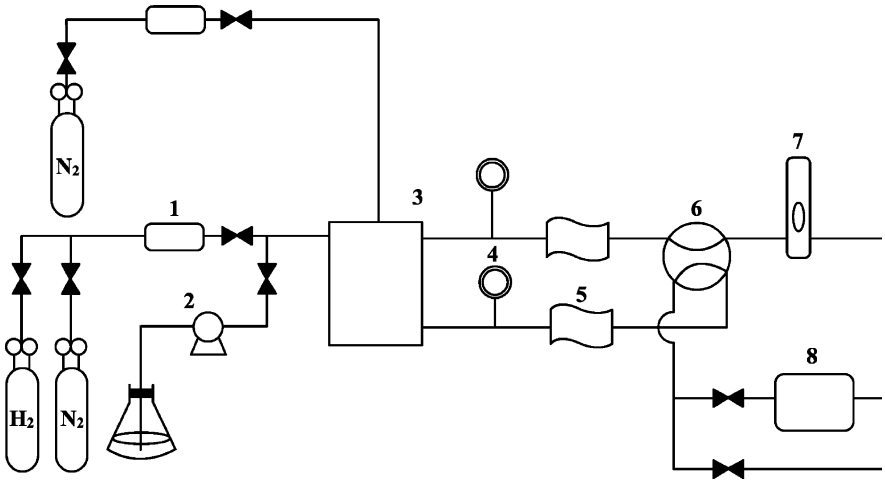

Fig. 1. A schematic diagram of the experimental apparatus for gas permeability measurement: (1) massflow controller, (2) poston metering pump, (3) membrane module, (4) pressure gauge, (5) back-pressure regulator, (6) six-pore valve, (7) bubble flowmeter, (8) gas chromatograph.

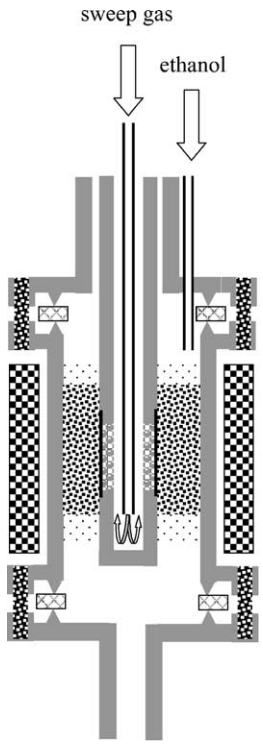

Fig. 2. Membrane reactor module: (▨) copper gasket; (▩) porous stainless steel; (▬) Pd–Ag membrane; (▨) silica powders; (▩) steel screw; (▩) stainless steel tube; (▩) furnace; (▩) catalysis bed.

3. Results and discussion

3.1. Deposition rate of palladium and silver

After surface activation, palladium nucleates have been doped in substrate surface. The reduction agent (N_2H_4) engaged in the redox reaction then N_2 would be released in the electroless plating process. The Ag or Pd content of Pd–Ag alloy membrane was calculated based on the weight gains. The thickness of the Pd–Ag film was determined by dividing the total weight gain by the plated surface area and the density of the alloy. The composition of Pd and Ag, thickness, roughness and permselectivity of each membrane are listed in Table 1. Fig. 3 shows the plating rates of palladium and silver as a function of time. Silver has a relatively low activity compared to palladium for the electroless plating process. It is well known that the electroless deposition of silver needs to be initiated by Pd nuclei. This was the reason that the silver was deposited after the deposition of the Pd film on the supports was completed. The amount of hydrazine could enhance both of Pd and Ag deposition rates. However Ag deposition rate was more efficiently increased than Pd when the amount of N_2H_4 was double.

3.2. Effect of calcinations

Fig. 4 shows the XRD patterns of Pd, Ag and Pd–Ag membranes before and after annealing. The reflection peaks of (1 1 1), (2 0 0) and (2 2 0) planes of Pd appeared at 2θ = 41.22°, 47.75° and 69.08°, and the (1 1 1), (2 0 0) and (2 2 0) planes of Ag peaked at 2θ = 39.15°, 45.32° and 65.37°. The reflection peak of heat-treated (723 K under H_2 atmosphere for 18 h) Pd or Ag membrane remained the same. In order to transform the deposited Pd–Ag into an alloy, the membrane was annealing at elevated temperature. The peaks of Pd–Ag membranes after annealing appeared at 2θ = 40.11°, 46.66° and 68.08°. All of these peaks are smooth and located between the reflection peaks of Pd (1 1 1) and Ag (1 1 1), Pd (2 0 0) and Ag (2 0 0), Pd (2 2 0) and Ag (2 2 0), respectively. This indicates that palladium and silver have formed a homogeneous alloy after annealing.

3.3. Ethanol dehydrogenation

The reactor used a porous stainless steel tube over which palladium and silver, with an overall thickness of ca. 29 μm, were electrolessly plated in sequence. In order to transform the deposited Pd–Ag into an alloy, the membrane was annealing at elevated temperature (723 K under H_2 atmosphere for 18 h). For the reaction test an industrial catalyst MDC-3 was load in the shell side of the membrane reactor.

The total reactions occurred in the reactor may include:

$$CH_3CH_2OH \rightarrow CH_3CHO + H_2, \quad \Delta H_f^{298} = 68.45\,kJ/mol \tag{1}$$

$$2CH_3CH_2OH \rightarrow C_2H_5OC_2H_5 + H_2O, \quad \Delta H_f^{298} = -25.35\,kJ/mol \tag{2}$$

$$2CH_3CH_2OH \rightarrow CH_3COOC_2H_5 + 2H_2, \quad \Delta H_f^{298} = 26.70\,kJ/mol \tag{3}$$

Table 1
The properties of Pd-based/PSS

Membrane	Composition (wt.%)		Thickness (μm)	Roughness (nm)	Permselectivity (J_{H_2}/J_{N_2})
	Pd	Ag			
M1	0	100	5.88	11.39	–
M2	100	0	10.00	36.47	2.5
M3	100	0	30.00	27.64	300
M4	18	82	15.77	14.65	–
M5	75	25	22.00	–	–
M6	78	22	29.00	25.63	∞

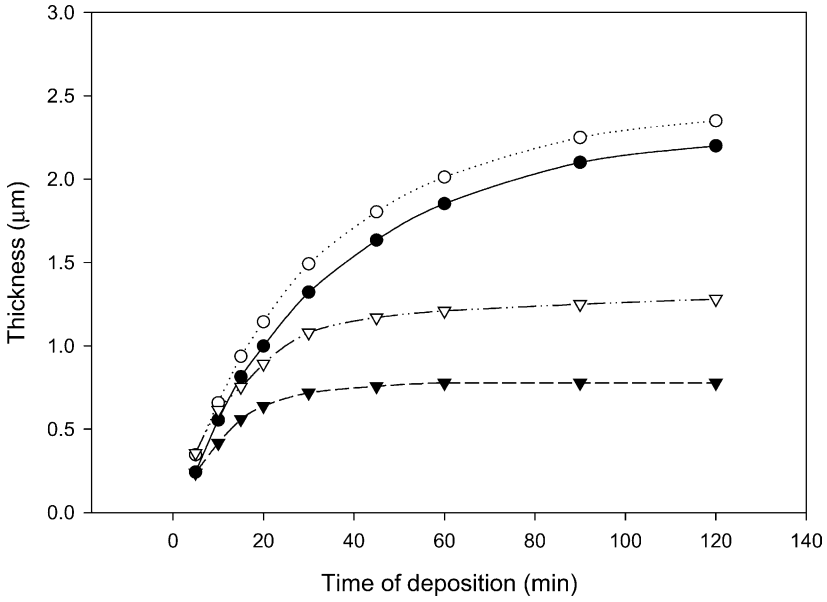

Fig. 3. Film growth as a function of plating time: (—●—) Pd deposition ($[N_2H_4] = 5.6 \times 10^{-3}$M); (···○··) Pd deposition ($[N_2H_4] = 1.1 \times 10^{-2}$M); (·—▼—·) Ag deposition ($[N_2H_4] = 5.6 \times 10^{-3}$M); (—▽·-) Ag deposition ($[N_2H_4] = 1.1 \times 10^{-2}$M).

$$CH_3CHO + CH_3CH_2OH \rightarrow CH_3COOC_2H_5 + H_2, \quad \Delta H_f^{298} = -41.75\,\text{kJ/mol} \tag{4}$$

If the reaction path follows $CH_3CH_2OH \rightarrow CH_3CHO \rightarrow CH_3COOC_2H_5$ (1 and 4), then the product of ethyl acetate decreases as the contact time will decrease due to the increasing ethanol fluxes. This infers that equations of (1) and (2) are competitive. If Eqs. (3) and (4) dominates ethyl acetate will increase as the contact time increases. This indicates that equations of (1), (2) and (3) are competitive.

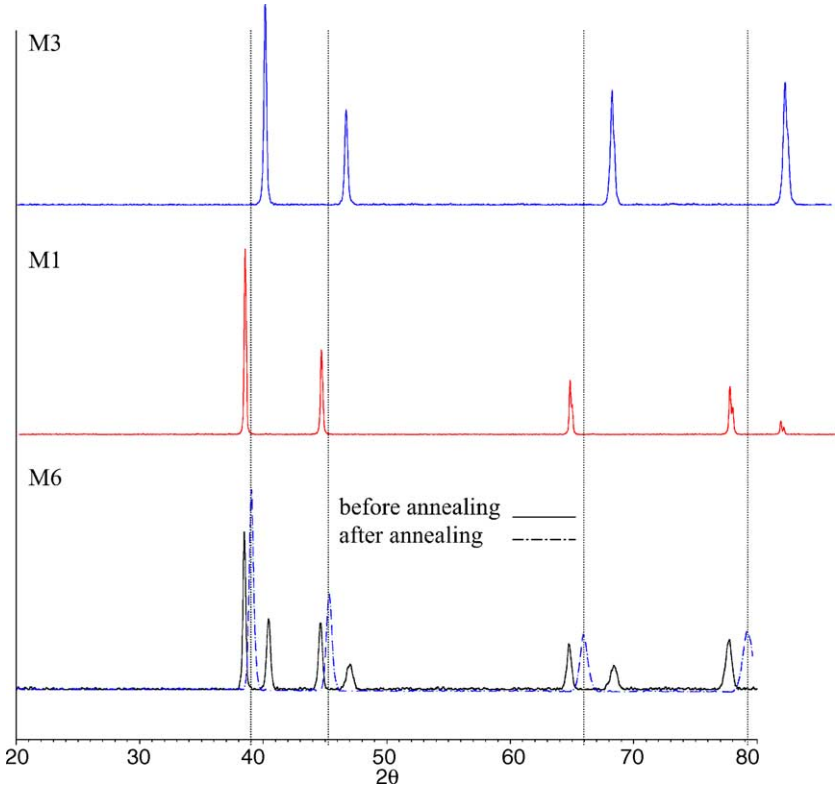

Fig. 4. XRD patterns of M1, M3 and M6 membranes before and after annealing.

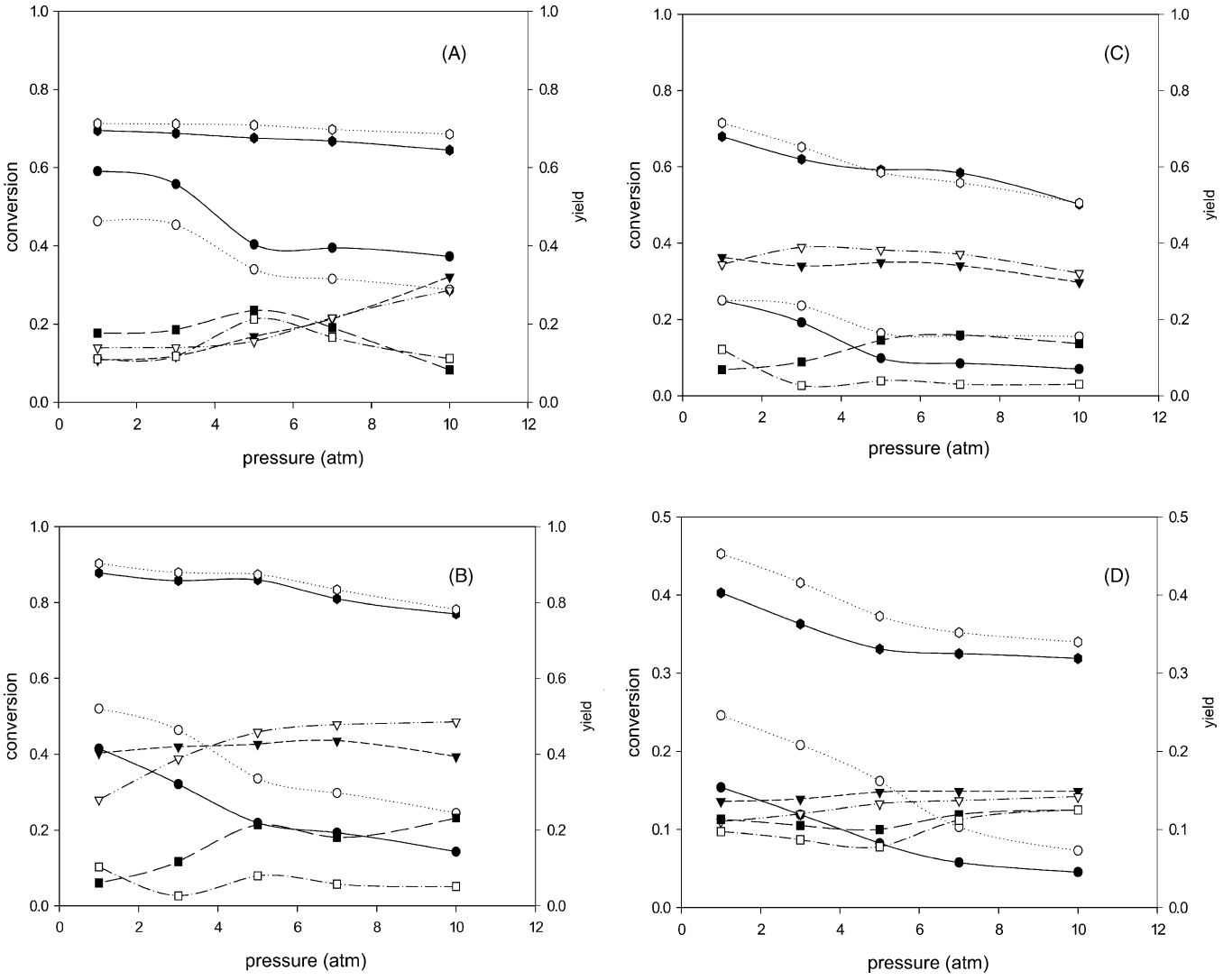

Fig. 5. Effect of transmembrane pressure on conversion of ethanol and yields of acetaldehyde, diethyl ether and ethyl acetate, with or without sweep gas (sweep gas flow rate = 9.22×10^{-1} mol/h) at (A) 723 K, WHSV = 3 h^{-1}; (B) 723 K, WHSV = 5 h^{-1}; (C) 623 K, WHSV = 3 h^{-1}; (D) 623 K, WHSV = 5 h^{-1}; $n_{N_2}/n_{C_2H_5OH} = 5.95$ for (A) and (C), $n_{N_2}/n_{C_2H_5OH} = 3.57$ for (B) and (D). Symbols: (⬢, ⬡) ethanol; (●, ○) acetaldehyde;(▼, ▽) diethyl ether; (■, □) ethyl acetate. Solid symbols denote no sweep gas and open symbols with sweep gas.

The results of experimental data were shown in Fig. 5. In Fig. 5(A) and (C) with WHSV = 3, when temperature was increased, conversion of ethanol and yields of acetaldehyde, diethyl ether and ethyl acetate increased. The same trend appeared at 623 K when WHSV was decreased (C and D). In (B) and (D) with WHSV = 5, when temperature was increased, conversion of ethanol and yield of acetaldehyde increased but the yields of diethyl ether and ethyl acetate did not show a systematic change. This indicates that at lower pressures or higher reaction temperature the reaction path was $2CH_3CH_2OH \rightarrow CH_3COOC_2H_5$ (1 and 3) and vice versa, the path of reaction was $CH_3CH_2OH \rightarrow CH_3CHO \rightarrow CH_3COOC_2H_5$ (1 and 4) at higher pressure and lower temperatures.

With a sweep gas in the permeation side, the hydrogen partial pressure in the permeation side decreases due to a dilution effect and the pressure difference across the membrane becomes larger, which therefore causes a higher hydrogen flux according to the Sieverts law. This boosts the dehydrogenation reaction to the product side and further increases the conversion, as shown in Fig. 5. In this study, with a definite amount of sweep gas (0.922 mol/h), the ethanol conversion attained 91.12%, which was closed to 100% and the discrepancy was attributed the insufficient flow rate of sweep gas compared to that of feed, otherwise, the ethanol conversion could reach 100%, as was predicted by Itoh for the dehydrogenation of cyclohexane [19].

Fig. 6 shows at different temperatures that the flow rates of hydrogen permeated through a Pd–Ag membrane varied with the flow rates of sweep gas. The H_2 fluxes increased with increasing flow rates of sweep gas and pressure. The

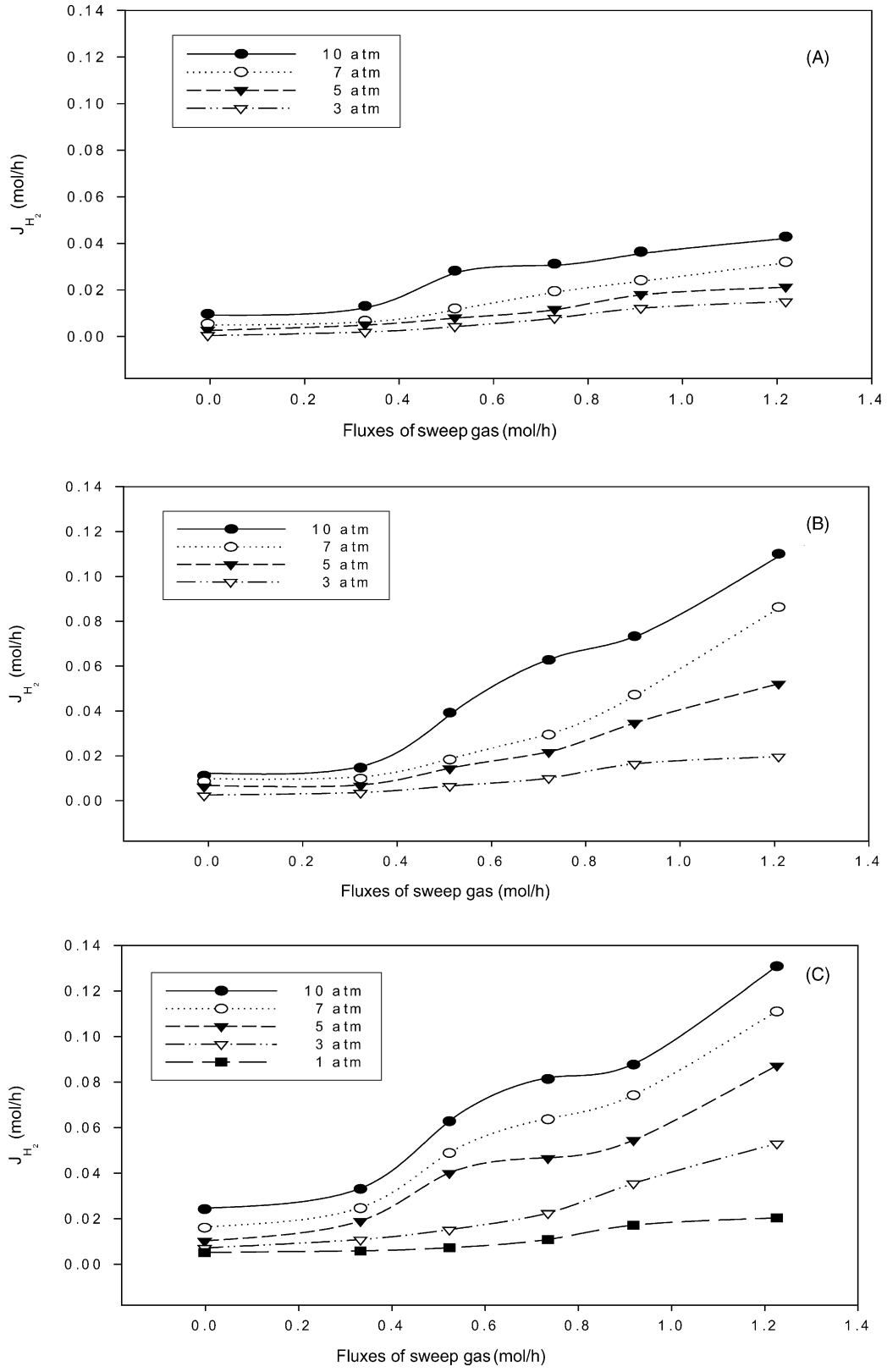

Fig. 6. The hydrogen permeation rates a function of sweep gas flow rates at (A) 623 K, (B) 673 K and (C) 723 K.

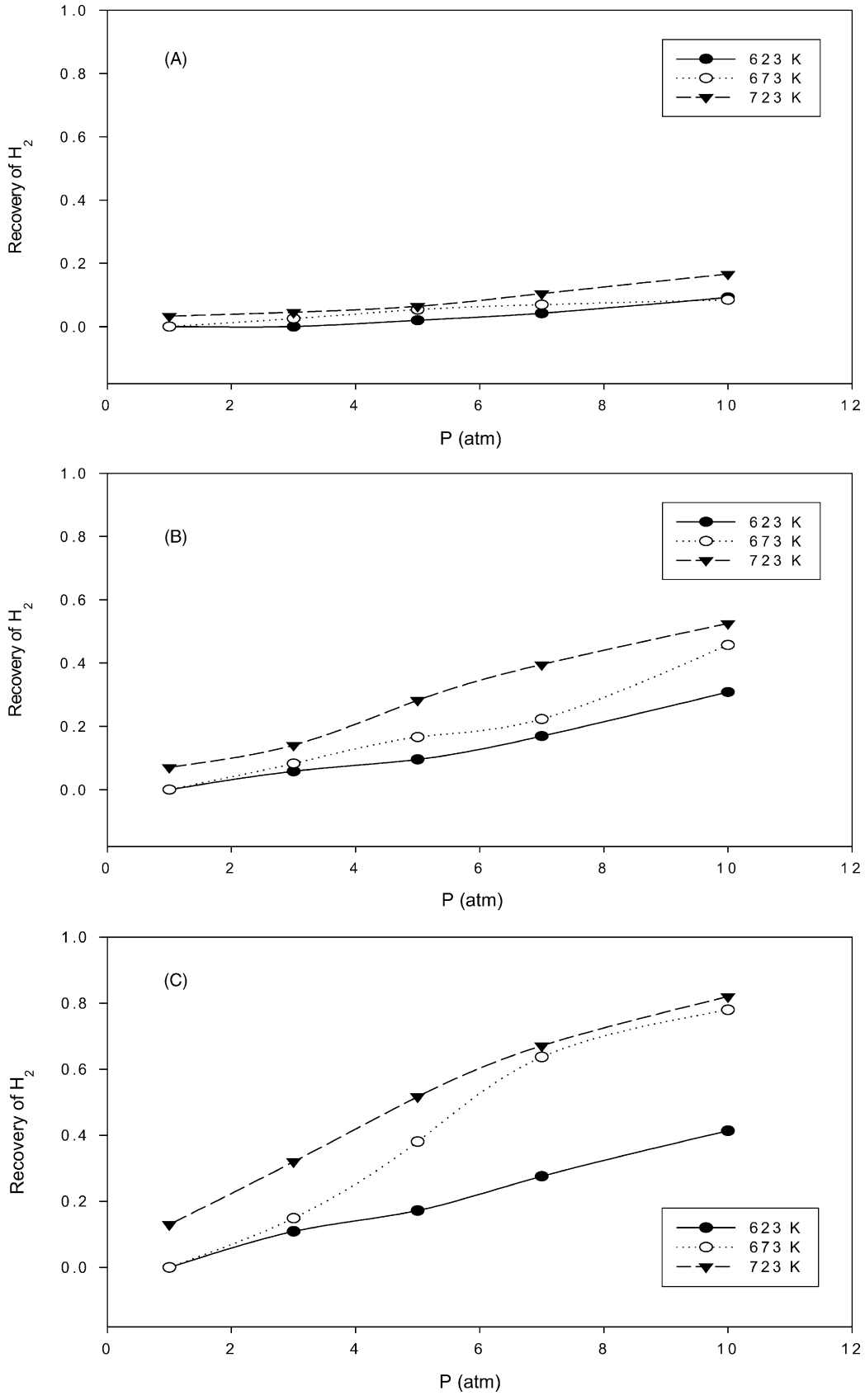

Fig. 7. Effect of transmembrane pressure on recovery of H_2: (A) without sweep gas, (B) with sweep gas = 0.738 mol/h and (C) with sweep gas = 1.23 mol/h.

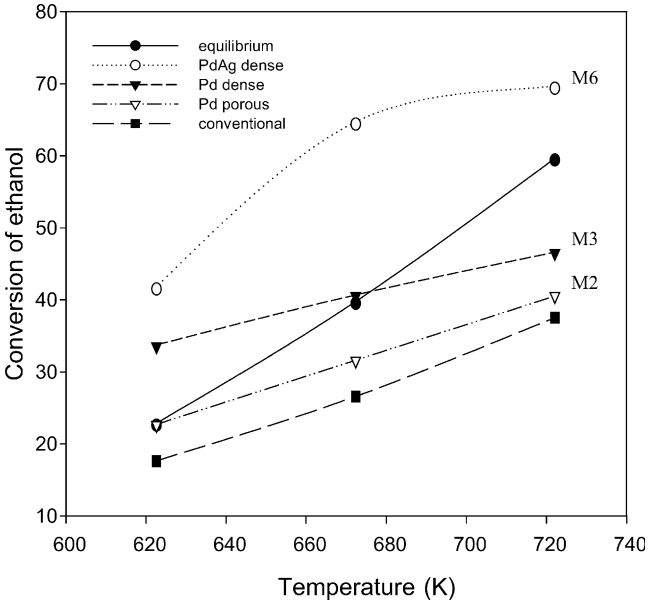

Fig. 8. Effect of reaction temperature on the conversion of ethanol in different reactors (reaction pressure = 10 atm).

effect of sweep gas on H_2 fluxes became remarkable at higher temperatures.

The effect of transmembrane pressure on the recovery of H_2 with a sweep gas is illustrated in Fig. 7. The recovery of H_2, defined as the amount of hydrogen extracted from the separation side per mole of hydrogen produced in the reaction side, increased linearly with increasing transmembrane pressures. The recovery of H_2 increased remarkably as the flow rate of sweep gas was increased from 0.738 mol/h to 1.23 mol/h, and more evidently at higher temperatures. These all conforms to the simulation results published previously [20].

The activity performance on dehydrogenation of ethanol to acetaldehyde was conducted in Pd and Pd–Ag alloy membrane reactors, at different reaction temperature and 10 atm and a conventional reactor was also tested for comparison. Fig. 8 shows that at 10 atm the ethanol conversion concordant with increasing temperature. Equilibrium conversion was also plotted for reference. The conversion of ethanol in the Pd membrane reactor was higher than that of in the conventional reactor, but the Pd–Ag alloy membrane reactor gave the highest conversion. The conversion of both of the latter two reactors exceeded the equilibrium value when temperature was below 673 K. This was due to the separation of hydrogen by permeation through a Pd-based membrane, so the thermodynamic equilibrium was allowed to displace to a new condition. Although the Pd porous membrane reactor performed better than the conventional reactor, its low hydrogen permselectivity still rendered the ethanol conversion to be lower than the equilibrium value.

Conclusions

Silver has a relative low activity compared to palladium for the electroless plating process. Thus, electroless deposition of silver needs to be initiated by Pd nuclei. This was the reason that the silver was deposited after the deposition of the Pd film on the supports was completed in sequential electroless plating process. The fluxes of H_2 increased with the increasing flow rates of sweep gas and transmembrane pressure. The effect of sweep gas advance H_2 fluxes was remarkable at higher temperatures. The recovery of H_2 increased with increasing the flow rate of sweep gas, the transmembrane pressure and the temperature. The Pd-based dense membrane reactors gave a higher conversion than thermodynamic equilibrium value for the dehydrogenation of ethanol.

Acknowledgements

This study was performed under the auspices of the National Science Council of the Republic of China, under contract number NSC91-2214-E-035-003, to which the authors wish to express their thanks.

Reference

[1] Y.M. Lin, G.L. Lee, M.H. Rei, Catal. Today 44 (1998) 343.
[2] Y.M. Lin, G.L. Lee, M.H. Rei, Int. J. Hydrogen Energy 25 (2000) 211.
[3] J.F. Deng, Z. Cao, B. Zhou, Appl. Catal. A 132 (1995) 9.
[4] Y. Cao, B.S. Liu, J.F. Deng, Appl. Catal. A 154 (1997) 129.
[5] B.A. Raich, H.C. Foley, Ind. Eng. Chem. Res. 37 (1998) 3888.
[6] G. Saracco, V. Specchia, Catal. Rev. Sci. Eng. 36 (1994) 305.
[7] E. Gobina, K. Hou, R. Hughes, Catal. Today 25 (1995) 365.
[8] J. She, B.P.A. Grandjean, S. Kaliaguine, Appl. Catal. A 119 (1994) 305.
[9] S. Uemiya, T. Matsuda, E. Kikuchi, J. Membr. Sci. 56 (1991) 315.
[10] S. Uemiya, Y. Kude, K. Sugino, N. Sato, T. Matsuda, E. Kikuchi, Chem. Lett. 10 (1988) 1687.
[11] S. Uemiya, N. Sato, H. Ando, Y. Kude, T. Matsuda, E. Kikuchi, J. Membr. Sci. 56 (1991) 303.
[12] S. Uemiya, T. Matsuda, E. Kikuchi, J. Membr. Sci. 56 (1991) 315.
[13] E. Kikuchi, S. Uemiya, Gas Sep. Purif. 5 (1991) 261.
[14] J.P. Collins, J.D. Way, Ind. Eng. Chem. Res. 32 (1993) 3006.
[15] J. Shu, B.P.A. Grandjean, E. Ghali, S. Kaliaguine, J. Membr. Sci. 77 (1993) 181.
[16] P.P. Mardilovich, Y. She, M.-H. Rei, Y.H. Ma, in: The Fourth International Conference on Inorganic Membranes, ICIM4-96, Gatlinburg, Tennessee, USA, 14–18 July, 1996.
[17] K.L. Yeung, A. Varma, AIChE J. 41 (1995) 2131.
[18] W.-H. Lin, H.-F. Chang, Flow mechanisms of hydrogen through Pd–Ag/PSS composite membrane, ChIChE J., submitted for publication.
[19] N. Itoh, AIChE J. 33 (1987) 1576.
[20] K.-Y. Chang, W.-H. Lin, H.-F. Chang, ChIChE J. 33 (2002) 225.